

An extremum principle of evaporation

Jingfeng Wang

Department of Civil and Environmental Engineering, Massachusetts Institute of Technology, Cambridge, Massachusetts, USA

Guido D. Salvucci

Department of Earth Sciences and Geography, Boston University, Boston, Massachusetts, USA

Rafael L. Bras

Department of Civil and Environmental Engineering, Massachusetts Institute of Technology, Cambridge, Massachusetts, USA

Received 9 February 2004; revised 4 May 2004; accepted 14 May 2004; published 9 September 2004.

[1] It is proposed, on the basis of an argument of thermodynamic equilibrium, that land-atmosphere interactive processes lead to thermal and hydrologic states of the land surface that maximize evaporation in a given meteorological environment. The extremum principle leads to general equations linking surface energy fluxes to surface temperature and soil moisture. The hypothesis of maximum evaporation has been tested with data from three field experiments. We found strong evidence suggesting that evaporation is maximized and furthermore that it is determined by the state variables (temperature, soil moisture, and sensible heat flux into the atmosphere) and relatively insensitive to water vapor pressure deficit. The theory allows an independent estimate of the coefficient in the Priestley-Taylor formula for potential evaporation, which is consistent with the widely accepted value of 1.26. *INDEX TERMS*: 3322 Meteorology and Atmospheric Dynamics: Land/atmosphere interactions; 1818 Hydrology: Evapotranspiration; 1836 Hydrology: Hydrologic budget (1655); 1878 Hydrology: Water/energy interactions; *KEYWORDS*: evaporation, extremum principle, surface heat fluxes, surface soil moisture, surface temperature

Citation: Wang, J., G. D. Salvucci, and R. L. Bras (2004), An extremum principle of evaporation, *Water Resour. Res.*, 40, W09303, doi:10.1029/2004WR003087.

1. Introduction

[2] Evaporation (conversion of liquid water into water vapor) is a unique hydrologic process that couples the dynamics of water and energy cycles over the Earth's surface. The foundation of the contemporary theory of evaporation is built on the pioneering work of Penman [1948]. Penman's theory has been playing a central role in parameterizing surface hydrology in climatic models over a wide range of time and space scales and vegetation conditions. It is impossible to summarize in this paper the vast number of publications by many research groups. One important text is the seminal monograph by Brutsaert [1982] that offers a paramount view of the subject. Over the past decades, advancement in the theoretical and observational study of evaporation after Penman has been achieved mainly with the help of the similarity theory [Obukhov, 1946; Businger *et al.*, 1971] in modeling water and heat transfer in the atmospheric boundary layer (ABL) as well as progress in experimental technologies such as the invention of the eddy correlation method [Dyer and Maher, 1965]. Fruitful results have been obtained on the effect of advection and atmospheric stability on the transport of water vapor [e.g., Bouchet, 1963; Brutsaert and Sticker,

1979; Mahrt and Ek, 1984; Katul and Parlange, 1992; Parlange and Katul, 1992] and on the interaction between the land surface and the boundary layer [McNaughton and Spriggs, 1986; Kim and Entekhabi, 1997], and comprehensive field experiments such as FIFE [Kanemasu *et al.*, 1992], HAPEX-SAHEL [Goutorbe *et al.*, 1994], and SGP (available at <http://hydrolab.arsusda.gov/sgp97/>), to name but a couple, have been performed.

[3] Vigorous discussions are still nevertheless ongoing about some of the fundamental concepts like potential evaporation. Raupach [2001] recently offered a comprehensive review of the concept of equilibrium evaporation and discussed some of the difficulties and contradictions still faced by the evaporation theory. The recent debate [Brutsaert and Parlange, 1998; Roderick and Farquhar, 2002] on the apparent paradox implied by decreasing pan evaporation observations around the world highlights the fact that misinterpretation of Penman's equation could lead to contrasting conclusions. Studies of climate [Delworth and Manabe, 1989] have found that accurate assessment of the water and energy balance at the land-atmosphere interface is crucial for modeling the Earth's climate system. A recent report by Pielke *et al.* [2002] further suggests that the surface energy budget may play a more important role than the carbon cycle in the climate at regional as well as global scales. Yet deficiencies in evaporation theory have hampered progress in understanding and modeling surface water

and energy balance. Accurate measurement and prediction of evaporation over the land surface remain daunting tasks [Desborough et al., 1996; Henderson-Sellers et al., 2003].

[4] Here we will seek to define an extremum principle behind the process of evaporation. The goal is to establish a self-contained theory of evaporation, in parallel with the classic similarity theory of water vapor transport in the ABL, that provides an alternative solution to the energy budget at the land-atmosphere interface. The theory emphasizes the energetics of phase change, and as such the (water vapor) transport mechanism is only one of the necessary conditions for the occurrence of evaporation. We start from the concept of thermodynamic equilibrium between two phases of a substance. A two-phase physical system often evolves at the fastest rate (or in the shortest time) toward a potential equilibrium state, and hence the evolution can be couched in terms of maximum (or minimum) principle. Early efforts in seeking extremum principles in various physical disciplines [e.g., Weinstock, 1952; Sieniutycz and Salamon, 1990; Ozawa et al., 2003] have revealed that nature often seeks efficient, optimal paths to potential equilibriums. Extension of this concept to the evaporation process over land surfaces would imply that liquid water in soil continuously evaporates, tending to saturate the air in contact with the soil. This eventual state of equilibrium would be reached, theoretically, as quickly as possible by maximizing the evaporation rate. It is widely accepted that the evaporation process consists of a climate-control stage followed by a soil-control stage depending on the soil moisture conditions [Jackson et al., 1976; Brutsaert, 1982; Salvucci, 1997]. The two-stage theory of evaporation implies that evaporation, at least during the climate-controlled stage, is largely controlled by meteorological environments. Although such treatment is useful in modeling the effect of soil moisture on evaporation, we will demonstrate that categorizing evaporation according to soil moisture conditions may not be necessary. Here we postulate and test the following hypothesis: Over a nonvegetated land surface the dynamics of water and heat exchange at the land-atmosphere interface leads to such surface hydrologic states that evaporation is always maximized under given conditions of radiative energy input, surface roughness, and physical properties of soil.

[5] Section 2 presents the theoretical development of the extremum principle. Section 3 focuses on testing the hypothesis of maximum evaporation by validating the governing equations derived in section 2 using observations from three field experiments. Section 4 illustrates the usefulness of the theory by estimating the empirical coefficient in the Priestley-Taylor formula for potential evaporation using the extremum principle. Conclusions and thoughts are given in section 5.

2. Theoretical Development

2.1. Physics of Evaporation

[6] The physics of evaporation has four essential elements: the supply of energy, the supply of water, fugacity (escaping tendency of liquid water molecules [e.g., Prausnitz, 1969]), and the turbulent transport mechanism. The source of energy for evaporation in natural Earth systems generally comes from solar radiation. Fugacity is measured by the saturated

vapor pressure at the liquid-vapor interface, which is determined by surface water temperature and water potential [Edlefsen and Anderson, 1943]. Water potential is functionally related to volumetric soil water content [e.g., Bras, 1990]. Supply of water depends on the soil wetness. The turbulent transport of water vapor (and heat) depends on wind speed and the thermal instability of the surface layer [Obukhov, 1946]. These physical processes associated with the four elements are well defined at the land-atmosphere interface. Here they are characterized by radiative fluxes, surface soil moisture, surface soil temperature, and turbulent sensible heat flux into the atmosphere, respectively. Therefore the rate of evaporation for a given radiative energy input corresponds to a particular combination of these state variables, i.e., surface soil moisture, surface soil temperature, and sensible heat flux, resulting from dynamic feedbacks among them through water and heat exchange across the land surface. Note that there are many combinations of ground, sensible heat fluxes, and evaporation that with net radiation could satisfy energy balance. We argue that the highly coupled land-atmosphere and the resulting feedback among the various processes actually favor a surface energy budget that maximizes evaporation.

[7] In the land-atmosphere system, atmospheric humidity is closely coupled with evaporation. Water vapor pressure deficit is often used in flux-gradient models of water vapor transport. Although strongly affected by synoptic advection of moisture, the near-surface vapor pressure deficit is potentially part of the feedback of the land-atmosphere system [e.g., Bouchet, 1963]: Greater evaporation increases the atmospheric humidity, which tends to reduce the gradient of water vapor pressure, leading to decreasing rate of evaporation. We will argue that the water vapor pressure deficit is a somewhat redundant variable of the evaporation function. We argue that this is because the land surface states contain the essential signal of near-surface atmospheric conditions as the result of strong land-atmosphere interaction.

2.2. Fluxes and the Surface State Variables

2.2.1. Evaporation (Latent Heat Flux)

[8] On the basis of discussion in section 2.1, the following fundamental variables are selected in the diagnostic equation of E : surface soil moisture θ_s , surface soil temperature T_s , and sensible heat flux into the atmosphere H at a given level of (radiative) energy input at the surface, R ,

$$E = E(\theta_s, T_s, H; R), \quad (1)$$

where other external parameters (defined as those not involving the land-atmosphere interaction dynamics) such as roughness of land surface are omitted for the sake of brevity. The justification of equation (1) without explicitly including water vapor pressure deficit will be discussed later in the paper. The theory development below will be independent of the functional form of E .

2.2.2. Ground Heat Flux

[9] It has been shown [Sellers et al., 1992; Wang and Bras, 1999] that ground heat flux G is determined by (the time history of) surface soil temperature and soil moisture,

$$G = G(T_s, \theta_s; R), \quad (2)$$

where T_s is a time series of soil temperature up to the current time of G . An analytical solution of G in terms of time history of T_s is given by *Wang and Bras* [1999]. The effect of soil moisture on G is included in soil properties [*de Vries*, 1963] through the thermal inertia parameter. The significance of including R as a parameter in equation (2) will be elucidated in section 3.

2.2.3. Sensible Heat Flux

[10] H is selected as an independent variable of E to represent the transport mechanism, one of the four essential elements of comparable importance for the evaporation process. Therefore H cannot be substituted mathematically by the other independent variables T_s and θ_s even though H , resulting from the combined effect of forced and free convection, is physically related to them. We believe that H is more appropriate than other choices such as the Monin-Obuhkov length or friction velocity in the similarity theories of turbulent transport [e.g., *Stull*, 1988]. Basically, equation (1) is a diagnostic equation analogous to the concept of the Bowen ratio where E is formulated diagnostically in terms of H (and moisture and temperature variables) but is not directly linked to any turbulent related parameters. In the linear nonequilibrium thermodynamics [e.g., *Kondepudi and Prigogine*, 1998, p. 351], heat fluxes are used as independent variables in formulating the entropy production function with the Onsager reciprocal relations. Furthermore, the choice of H as a state variable explicitly leads to partition of radiative input as a result of the optimization without specifying specific models for H . This nonparametric formulation allows the central hypothesis to be tested without specifying a turbulence transport model and its parameters. Indeed, modeling turbulence is irrelevant to the validity of the hypothesis.

2.3. The Extremum Principle of Evaporation

[11] The maximized E and the associated optimal surface fluxes and state variables can be obtained by solving a maximization problem with an imposed constraint of surface energy balance,

$$E \equiv \max\{E(\theta_s, T_s, H; R) \mid E + H + G = R_n\} \quad \forall(\theta_s, T_s, H), \quad (3)$$

where R_n is the net radiation at the surface, and the ‘‘for all’’ symbol means for all possible combinations (of the independent variables θ_s , T_s , and H). R_n has short-wave and long-wave radiation components,

$$R_n = R^{\text{sd}} - R^{\text{su}} + R^{\text{ld}} - R^{\text{lu}}, \quad (4)$$

where R^{sd} is the incoming short-wave radiation, R^{su} is the reflected short-wave radiation, R^{ld} is the downward long-wave radiation, and R^{lu} is the emitted long-wave radiation from the surface. All terms except R^{sd} are affected by surface temperature and soil moisture.

[12] The optimization of E , according to equation (3), may be carried out in various ways depending on the specification of parameter R . We will study three cases of given R parameter: (1) $R = R_n - G$, (2) $R = R_n$, and (3) $R = R^{\text{sd}}$. The first case of given nonturbulent energy flux (available energy) reveals the turbulent energy budget, a feature commonly described by the Bowen ratio. The second case elucidates the partition of net radiation into heat fluxes of latent, sensible, and ground. The third case deals with the budget of all the surface energy fluxes.

[13] It is important to emphasize that equation (3) is a unique statement of energy balance. Given a level of energy input, what this hypothesis argues is that there is a unique partitioning of that energy into the various surface fluxes. That partitioning is predicated on the land-surface atmosphere tendency to achieve thermodynamic equilibrium as quickly as possible. Clarity in this concept will help to understand why the formulation is not explicitly dependent on near-surface atmospheric moisture.

2.4. Governing Equations

[14] The Lagrangian multiplier method is used to derive the governing equations for E . Maximum E corresponds to vanishing partial derivatives of its Lagrangian function with respect to all independent variables including the Lagrangian multiplier. The Lagrangian function f may be defined as

$$f(\theta_s, T_s, H, \lambda; R) \equiv E(\theta_s, T_s, H; R) + \lambda[R_n - E(\theta_s, T_s, H; R) - H - G(\theta_s, T_s; R)], \quad (5)$$

where λ is the Lagrangian multiplier. The Lagrange multiplier method will select, among all possible combinations of T_s , θ_s , and H that satisfy the surface energy balance, the optimal solutions of T_s , θ_s , and H that maximize E .

2.4.1. Given Available Energy $R_n - G$

[15] Differentiating f in equation (5) with respect to θ_s , T_s , H , and λ and setting the corresponding (partial) derivatives to zero while keeping $R = R_n - G$ constant lead to

$$\frac{\partial f}{\partial T_s} \Big|_{\theta_s, H, \lambda}^{R=R_n-G} \equiv \frac{\partial E}{\partial T_s} \Big|_{\theta_s, H}^{R=R_n-G} + \lambda \left(- \frac{\partial E}{\partial T_s} \Big|_{\theta_s, H}^{R=R_n-G} \right) = 0 \quad (6)$$

$$\frac{\partial f}{\partial \theta_s} \Big|_{T_s, H, \lambda}^{R=R_n-G} \equiv \frac{\partial E}{\partial \theta_s} \Big|_{T_s, H}^{R=R_n-G} + \lambda \left(- \frac{\partial E}{\partial \theta_s} \Big|_{T_s, H}^{R=R_n-G} \right) = 0 \quad (7)$$

$$\frac{\partial f}{\partial H} \Big|_{\theta_s, T_s, \lambda}^{R=R_n-G} \equiv \frac{\partial E}{\partial H} \Big|_{\theta_s, T_s}^{R=R_n-G} + \lambda \left(- \frac{\partial E}{\partial H} \Big|_{\theta_s, T_s}^{R=R_n-G} - 1 \right) = 0 \quad (8)$$

$$\frac{\partial f}{\partial \lambda} \Big|_{\theta_s, T_s, H}^{R=R_n-G} \equiv (R_n - G) - E - H = 0, \quad (9)$$

where the superscripts specify the given parameter and the subscripts emphasize the nondifferentiating independent variables of the dependent variables. T_s here is the temperature at the current time of the flux variables. The above equations yield

$$\frac{\partial E}{\partial T_s} = 0 \quad (10)$$

$$\frac{\partial E}{\partial \theta_s} = 0 \quad (11)$$

$$R_n - G = E + H \quad (12)$$

$$\lambda = \left[1 + \left(\frac{\partial E}{\partial H} \right)^{-1} \right]^{-1}, \quad (13)$$

where the given parameter $R = R_n - G$ in the superscripts and the nondifferentiating independent variables in the subscripts are omitted for conciseness. Keep in mind that all derivatives in equations (10)–(13) are understood as under the condition of given $R = R_n - G$. The derivative for a certain given R is referred to as a conditional derivative hereinafter.

[16] Equations (10)–(12) are used to solve for an optimal solution of θ_s , T_s , and H that maximizes E . For the case of given $R_n - G$, the optimal solution of θ_s and T_s (i.e., observed values of θ_s and T_s) has been implicitly included in G and the radiative flux terms in equation (4). Interestingly, maximizing E without the energy constraint leads to the same equations as (10) and (11). However, vanishing derivatives of E with respect to θ_s and T_s are only possible with limited energy supply. Unconditional derivatives of E with respect to T_s and θ_s are positive since greater fugacity or water supply will always enhance evaporation.

2.4.2. Given Net Radiation R_n

[17] Differentiating f in equation (5) with respect to θ_s , T_s , H , and λ and setting the corresponding (partial) derivatives to zero while keeping $R = R_n$ constant lead to

$$\left. \frac{\partial f}{\partial T_s} \right|_{\theta_s, H, \lambda}^{R=R_n} \equiv \left. \frac{\partial E}{\partial T_s} \right|_{\theta_s, H}^{R=R_n} + \lambda \left(- \left. \frac{\partial E}{\partial T_s} \right|_{\theta_s, H}^{R=R_n} - \left. \frac{\partial G}{\partial T_s} \right|_{\theta_s, H}^{R=R_n} \right) = 0 \quad (14)$$

$$\left. \frac{\partial f}{\partial \theta_s} \right|_{T_s, H, \lambda}^{R=R_n} \equiv \left. \frac{\partial E}{\partial \theta_s} \right|_{T_s, H}^{R=R_n} + \lambda \left(- \left. \frac{\partial E}{\partial \theta_s} \right|_{T_s, H}^{R=R_n} - \left. \frac{\partial G}{\partial \theta_s} \right|_{T_s, H}^{R=R_n} \right) = 0 \quad (15)$$

$$\left. \frac{\partial f}{\partial H} \right|_{\theta_s, T_s, \lambda}^{R=R_n} \equiv \left. \frac{\partial E}{\partial H} \right|_{\theta_s, T_s}^{R=R_n} + \lambda \left(- \left. \frac{\partial E}{\partial H} \right|_{\theta_s, T_s}^{R=R_n} - 1 \right) = 0 \quad (16)$$

$$\left. \frac{\partial f}{\partial \lambda} \right|_{\theta_s, T_s, H}^{R=R_n} \equiv R_n - E - H - G = 0. \quad (17)$$

The governing equations for E now become

$$\frac{\partial E}{\partial T_s} = \frac{\partial E}{\partial H} \frac{\partial G}{\partial T_s} \quad (18)$$

$$\frac{\partial E}{\partial \theta_s} = \frac{\partial E}{\partial H} \frac{\partial G}{\partial \theta_s} \quad (19)$$

$$R_n = E + H + G \quad (20)$$

$$\lambda = \left[1 + \left(\frac{\partial E}{\partial H} \right)^{-1} \right]^{-1}. \quad (21)$$

It is important to emphasize again that all derivative terms in equations (18) and (19) are conditional derivatives for a given $R = R_n$. The given parameter $R = R_n$ in the superscripts and the nondifferentiating variables in the subscripts are again omitted for brevity. Like the previous case, given $R = R_n$ assumes that the optimal solution of T_s and θ_s is implicitly reflected in the

observed R_n in equation (20) although the individual values of T_s and θ_s remain unspecified at the moment.

[18] Equations (18) and (19) reveal how the three components of the surface energy balance compete for the net radiative energy flux to maximize evaporation. Equation (18) indicates that the enhancement of evaporation due to higher surface temperature (or greater fugacity) is proportional to that due to enhanced turbulent transport. The relative magnitudes are determined by the conductive heat loss into the soil. This feature highlights the role of land surface in the partition of net radiation into surface heat fluxes since ground heat flux is closely related to the soil properties. Therefore heat and/or water transfer in the soil layer play a critical role in the water and heat exchange across the land surface.

2.4.3. Given Solar Radiation R^{sd}

[19] Contrary to the previous two cases where the effect of the surface conditions on the given parameter R_n is implicitly represented by the optimal solutions of θ_s and T_s , R^{sd} as the given parameter is independent of the surface variables. Consequently, maximum E and the associated surface fluxes and variables are solved under the least restrictive constraint. Theoretically, all other radiative fluxes in equation (4) are related to the surface variables. Soil moisture has an appreciable effect on albedo or reflected solar radiation [Idso *et al.*, 1975]. Emitted long-wave radiation from the surface is a strong function of surface temperature. Downward long-wave radiation is a function of integrated atmospheric temperature and moisture profiles, which are closely coupled with the surface conditions.

[20] Following the above procedure and assuming the dependence of R^{su} , R^{ld} , and R^{ld} on θ_s and T_s , the governing equations for E given incoming short-wave radiation are

$$\frac{\partial E}{\partial T_s} = \frac{\partial E}{\partial H} \left[\frac{\partial G}{\partial T_s} + \frac{\partial R^{su}}{\partial T_s} + \frac{\partial (R^{lu} - R^{ld})}{\partial T_s} \right] \quad (22)$$

$$\frac{\partial E}{\partial \theta_s} = \frac{\partial E}{\partial H} \left[\frac{\partial G}{\partial \theta_s} + \frac{\partial R^{su}}{\partial \theta_s} + \frac{\partial (R^{lu} - R^{ld})}{\partial \theta_s} \right] \quad (23)$$

$$R^{sd} = E + H + G + R^{su} - R^{ld} + R^{lu} \quad (24)$$

$$\lambda = \left[1 + \left(\frac{\partial E}{\partial H} \right)^{-1} \right]^{-1}. \quad (25)$$

Once again, all the derivatives in the above equations are conditioned on a given $R = R^{sd}$.

[21] Equations (22)–(24) provide the most general description of partition of solar radiation into turbulent and nonturbulent energy fluxes to maximize evaporation. Here we only assume the radiative fluxes R^{su} , R^{lu} , and R^{ld} in equations (22)–(24) are functions of T_s and θ_s , but no specific models are used. Once E , G , R^{su} , R^{lu} , and R^{ld} are parameterized in terms of T_s and θ_s , equations (22)–(24) yield an optimal solution of all surface energy fluxes and surface temperature and soil moisture that maximizes E .

[22] The three sets of governing equations based on the extremum principle of evaporation shed new light on the land-atmosphere interaction. Equations (10)–(12) describe the detailed balance between the turbulent fluxes. Equations (18)–(20) further reveal the partition of net radiation into turbulent and conductive heat fluxes. They highlight

the role of land surface in the energy balance through the ground heat flux term. Ground heat flux is often considered of secondary importance compared with the turbulent heat fluxes. Equations (18)–(20) suggest that ground heat flux plays an equally important role to that of the turbulent fluxes in the exchange of water and heat at the surface. Equations (22)–(24) provide a comprehensive description of surface energy balance by linking all conductive, turbulent, and radiative energy fluxes to the surface temperature and soil moisture states.

3. Test of the Hypothesis

[23] The hypothesis was tested by validating the three sets of governing equations obtained in the previous section. The main task is to calculate the conditional derivatives appearing in the extremality expressions.

3.1. Calculation of the Conditional Derivatives

[24] Time series measurements of surface heat fluxes and surface soil moisture and temperature have to be used to calculate the conditional derivatives. The first step in calculating the conditional derivatives is to translate the time series measurements from field experiments into new sequences. The new sequences are obtained by rearranging all the measured time series variables in the ascending (or descending) order of the given parameter R . For example, we may sort the original time series in the ascending order of R_n for calculating the conditional derivatives in equations (18) and (19). Then the resulting sequences are divided into a number of subsequences with equal number of data points. Now these new subsequences are conditioned within a narrow range of a certain given R .

[25] The conditional derivatives of a flux variable can be obtained from the regression coefficients of a first-order approximation of its total differential. We use E as an example to illustrate the algorithm. According to equation (1), we can write the total differential of E as

$$E^i - E^0 = \frac{\partial E}{\partial T_s} (T_s^i - T_s^0) + \frac{\partial E}{\partial \theta_s} (\theta_s^i - \theta_s^0) + \frac{\partial E}{\partial H} (H^i - H^0) \quad (26)$$

$i = 1, 2, \dots, m,$

where superscript 0 stands for a reference point of a subsequence at which the derivatives are defined, i is the i th point of a certain subsequence, and m is the number of data points in the subsequence. The derivatives of other energy fluxes including G , R^{su} , and R^{lu} are calculated in the same manner except that H is not an independent variable of these fluxes. A linear regression procedure will be used to obtain the three derivative terms in equation (26) from m equations ($m > 3$). Since equation (26) is linear in the unknowns (derivatives), the reference points T_s^0 , θ_s^0 , and H^0 need not be specified.

3.2. Data

3.2.1. HAPEX-SAHEL

[26] Data from the Hydrology-Atmosphere Pilot Experiment in the Sahel experiment (1990–1992) [Goutorbe *et al.*, 1994] are used in this study (Figure 1). The Southern Supersite Tiger Bush site (13°11.89'N, 2°14.37'E) is located in a bare soil region where turbulent heat fluxes were measured. Ground heat flux was derived from measure-

ments of soil heat flux plates and temperature probes. The heat fluxes and soil temperature data have a 20-min and 10-min resolution, respectively. Surface soil moisture was sampled daily. An interpolation procedure was carried out to create a series of soil moisture sequences to match the temporal resolution of the other variables. Obviously, such a derived soil moisture sequence does not resolve its diurnal variability. Nevertheless, the derived product does cover the entire spectrum of soil moisture ranging from saturation to nearly dry. Over the period of 3–24 September 1992, the soil experienced several wetting-drying cycles followed by a long drying-down period. Depending on the given energy supply parameter, the time series shown in Figure 1 will be rearranged to produce three different sequences (not shown) to calculate the corresponding conditional derivatives.

3.2.2. SGP97

[27] Data from the Southern Great Plains '97 field experiment (data are available online at http://daac.gsfc.nasa.gov/CAMPAIGN_DOCS/SGP97/sgp97.html) will also be used in the hypothesis test, but limited to evaluate equations (10) and (18). (Readers are referred to <http://hydrolab.arsusda.gov/sgp97> for a complete description of the field experiment.) The measured surface heat fluxes and air temperature are illustrated in Figure 2. This site (central facility CF01) is located in an area partially covered by grazed pasture with significant bare soil exposed. There were a number of rain events through the observation period. Surface soil moisture was assumed to stay at a relatively high level with reduced diurnal variability, as the continuous record of surface soil moisture is not available. Near-surface air temperature is used to obtain missing surface (soil) temperature exploiting the cross correlation between them. Although less ideal, this data set is valuable as a second site to test the hypothesis.

3.2.3. University of California, Davis

[28] A field experiment was conducted at the University of California, Davis, in 1990. The research site was located within a bare soil region. The soil was kept wet by an irrigation system. Two lysimeters (weighting and floating) were used to measure evaporation on a 20-min basis. Ground heat flux was measured with two soil heat flux plates installed 0.5 cm below the surface. Skin temperature was not measured. Near-surface air temperature at 0.8 m above the surface will be used instead. Other measurements include net radiation, wind speed, relative humidity, etc., all sampled at 20-min intervals. Since sensible heat flux was not directly measured, it will be calculated as the residual of surface energy balance. The measured variables used in this analysis are shown in Figure 3. We select Julian days 257, 297, 324, and 351, which correspond to the moist surface conditions (i.e., near-saturated surface soil moisture conditions according to Parlange and Katul [1992]). Only positive lysimeter data points are used here. Readers are referred to Katul and Parlange [1992] for a full description of the experiment.

3.3. Results

3.3.1. The HAPEX-SAHEL Site

3.3.1.1. Given $R_n - G$

[29] The histograms of the two conditional derivatives in equations (10) and (11) are illustrated in Figure 4. Each of the derivatives has values concentrated within a narrow

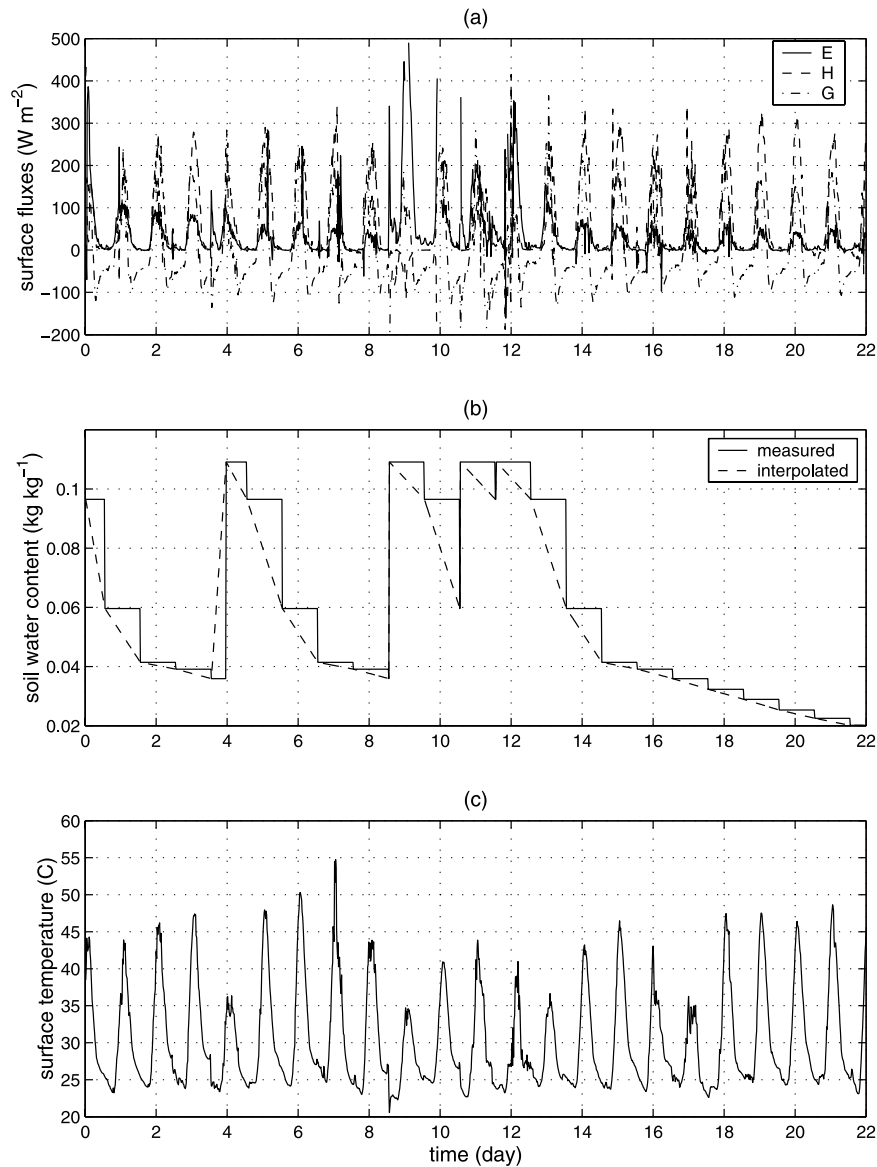


Figure 1. (a) Surface heat fluxes, E , H , and G (W m^{-2}). (b) Soil water content, θ_s , ($\text{kg (H}_2\text{O)} (\text{kg (soil))}^{-1}$). (c) Surface temperature, T_s ($^{\circ}\text{C}$). Measurements from HAPEX-SAHEL experiment at a bare soil site, 3–24 September 1992. See color version of this figure in the HTML.

domain around zero. “Zero” is defined relative to a reference called “nominal” value. As shown in Figure 1, a $\sim 100 \text{ W m}^{-2}$ change in E corresponds to a $\sim 10^{\circ}\text{K}$ change in T_s . Therefore the nominal value of the partial derivative E_{T_s} is $\sim 10 \text{ W m}^{-2} \text{ K}^{-1}$, which is 3 orders of magnitude greater than the mean E_{T_s} given $R_n - G$, $\sim 0.01 \text{ W m}^{-2} \text{ K}^{-1}$ (see Figure 4a). Similarly, the “nominal” value of the partial derivative E_{θ_s} , $\sim 10^3 \text{ W m}^{-2}$, is also 3 orders of magnitude greater than the mean E_{θ_s} given $R_n - G$, $\sim 1 \text{ W m}^{-2}$ (see Figure 4b). We conclude that the derivatives are equal to zero as predicted by equations (10) and (11). We note that the quality of the soil moisture data (interpolated from daily observations) has little negative impact on the calculation of E_{θ_s} under the condition of given $R_n - G$. This feature may be attributed to the fact that observed G contains a strong signal of soil moisture that compensates the errors in the interpolated soil moisture series.

3.3.1.2. Given R_n

[30] The validity of equation (18) is clearly demonstrated by Figure 5a visually and statistically. Linear functions analysis [e.g., *Davies and Goldsmith, 1984*] yields a mean slope $\bar{b} = 0.883$ with 95% confidence interval of \bar{b} (1.041, 0.731) (see Figure 5a), suggesting the calculated temperature derivatives follow the relationship predicted in equation (18). The result is robust, as the close agreement between the both sides of equation (18) is not affected by the bin size (i.e., the number of data points in computing the regression coefficients). The validity of equation (19) is also suggested by Figure 5b, although the statistical analysis shows a moderate bias in the mean slope in the moisture derivative terms. The poorer result exhibited in the validation of soil-moisture-related conditional derivatives (Figure 5b) compared to the temperature-related conditional derivatives (Figure 5a) is likely due to the lack of diurnal

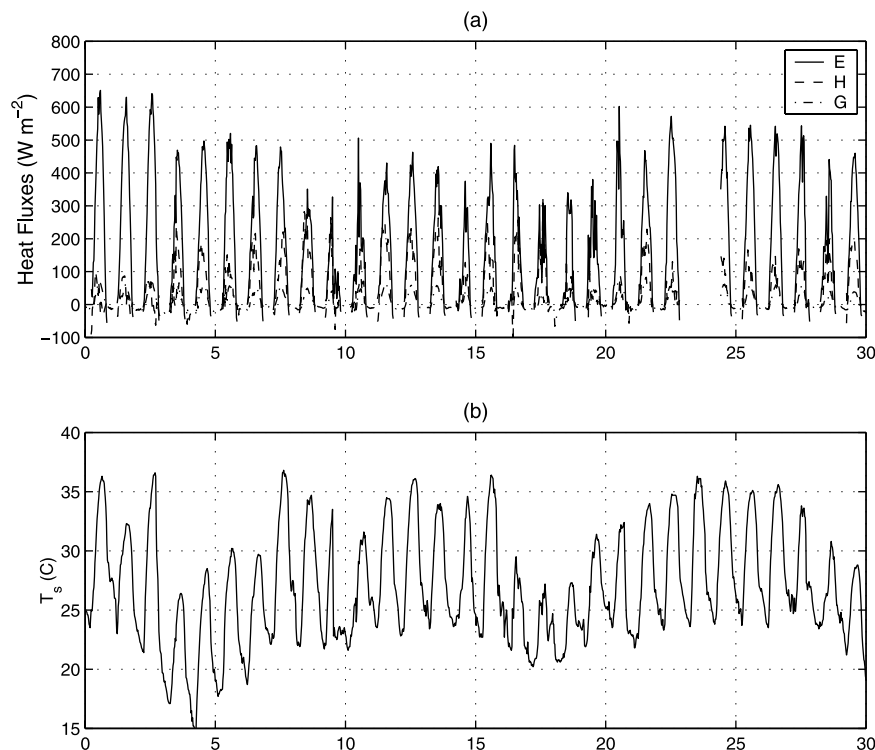


Figure 2. (a) Surface heat fluxes (W m^{-2}). (b) Surface (air) temperature ($^{\circ}\text{C}$). Measurements from SGP97 experiment at the CF01 ARM2 site, 1–30 July 1997. See color version of this figure in the HTML.

variability in the interpolated soil moisture data. Furthermore, the signal of soil moisture contained in R_n is probably not strong enough to correct the errors in the interpolated soil moisture series. Nonetheless, the test based on this data set presents encouraging evidence in support of equations (18) and (19).

3.3.1.3. Given R^{sd}

[31] Observed radiative fluxes R^{su} and R^{ld} (not shown) are used to compute the conditional derivatives in equations (22) and (23). Since the data set does not provide direct measurements of emitted long-wave radiation from the surface, R^{lu} is parameterized as $R^{lu} = \epsilon\sigma T_s^4$ where surface emissivity ϵ is assumed to be 0.98 and σ is the Stefan-Boltzmann's constant. Figure 6a suggests the validity of equation (18) according to the statistics. A regression analysis gives a mean regression slope $\bar{b} = 0.738$ with 95% confidence interval of \bar{b} (1.034, 0.467). These computed derivatives have greater bias and scatter than those for the case of given R_n (Figure 5a). A likely cause is that the added derivative terms in equation (22) compared with equation (18) introduce extra estimation errors. Nonetheless, this data set offers positive evidence to support equation (22). Justification of equation (23) based on the statistics may be inconclusive, although Figure 6b is visually suggestive. Regression analysis leads to a relatively large bias in the mean slope ($\bar{b} = 0.261$). We contend that a definite conclusion will require more accurate soil moisture measurements.

[32] Note that models of the surface energy fluxes (except for emitted long-wave radiation due to lack of direct measurements) were not assumed. In other words, the test of the hypothesis is model-independent, meaning it is not affected by the parameterizations of turbulent transport in

the ABL. Model independence makes the test of the hypothesis powerful and convincing since the results are robust and generalizable. We realize that the three sets of governing equations are the necessary, instead of the sufficient, conditions for E to be maximum (as opposed to a minimum). Nevertheless, the physics of evaporation discussed earlier in this paper makes it plausible to argue that E described by these equations should be maximum.

3.3.2. The SGP97 Site

[33] The test presented below offers a partial evaluation of the governing equations derived in section 2.4. Since the desired measurement of surface soil moisture is not available, the θ_s related term cannot be included in equation (26) to calculate the other derivative terms in equations (10) and (18), and equations (11) and (19) cannot be tested at all at this location. Measurements of individual long- and short-wave radiative fluxes are not available to test the governing equations for the case of given R^{sd} .

3.3.2.1. Given $R_n - G$

[34] The histogram of the derivatives in equation (10) is displayed in Figure 7. The estimated derivatives are confined within narrow ranges centered around the theoretical value of zero. The calculated mean of the conditional $\partial E/\partial T_s \sim 0.004 \text{ W m}^{-2} \text{ K}^{-1}$ is 4 orders of magnitudes smaller than the corresponding nominal value. Consequently, the derivative is statistically equal to zero. The test supports the validity of equation (10).

3.3.2.2. Given R_n

[35] The validity of equation (18) is evident visually and statistically with $\bar{b} = 1.02$ and the 95% confidence interval of $\bar{b} = [1.14, 0.88]$ (Figure 8). Remember that the test used near-surface air temperature as a substitute when surface soil temperature is unavailable.

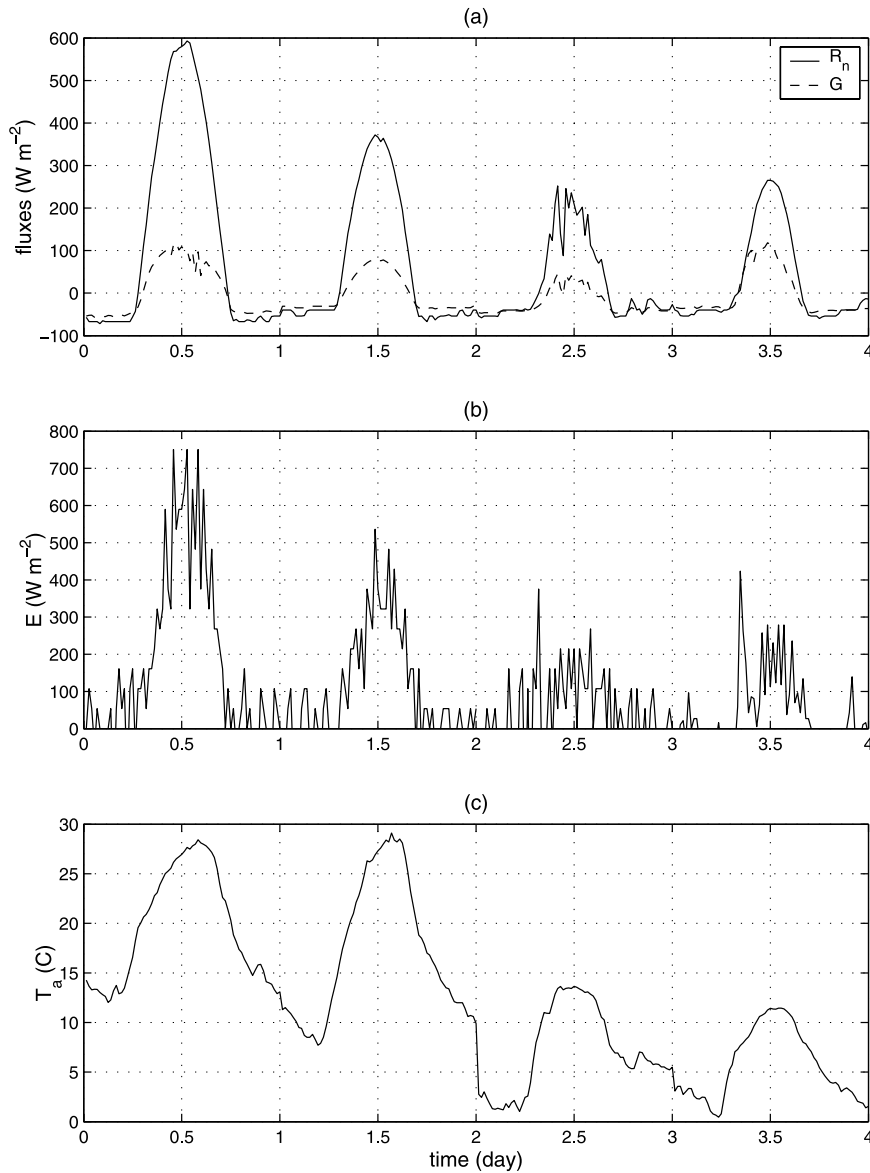


Figure 3. Observations demonstrated consecutively under moist surface conditions. (a) Surface heat fluxes. (b) Evaporation from the weighting lysimeter. (c) Near-surface air temperature. The Campbell field at the University of California, Davis, Julian days 257, 297, 324, and 351, 1990. See color version of this figure in the HTML.

3.3.3. The University of California, Davis, Site

[36] Test of the hypothesis is limited to validating equation (18) since equation (19) becomes trivial over saturated soil. The noisy lysimeter data (see Figure 3b) further limit the test to the case of given R_n . The cases of given $R_n - G$ and R^{ns} will not be tested due to the lack of measurements of H and R^{ld} . Again, Figure 9 offers good visual and statistical evidence of the validity of equation (18).

3.4. Justification of Equation (1)

[37] It is widely known that evaporation can be estimated using the water vapor pressure deficit v_d as an independent variable. Yet the development of our theory assumes E is a function of surface variables only. The physical basis of this argument is that the effect of atmospheric conditions on

evaporation has been represented by the surface variables due to the strong interaction between the land and the atmosphere. Here we offer a mathematical proof using the parameter restriction methodology combined with the meta-analysis technique [e.g., Schulze *et al.*, 2003]. The statistical analysis will tell us whether including the water vapor deficit v_d as an additional independent variable of E ,

$$E = E(\theta_s, T_s, H, v_d; R), \quad (27)$$

leads to significant improvement of the predictability compared to that of equation (1). The null hypothesis under test, H_0 , is that v_d does not significantly increase the predictability of evaporation.

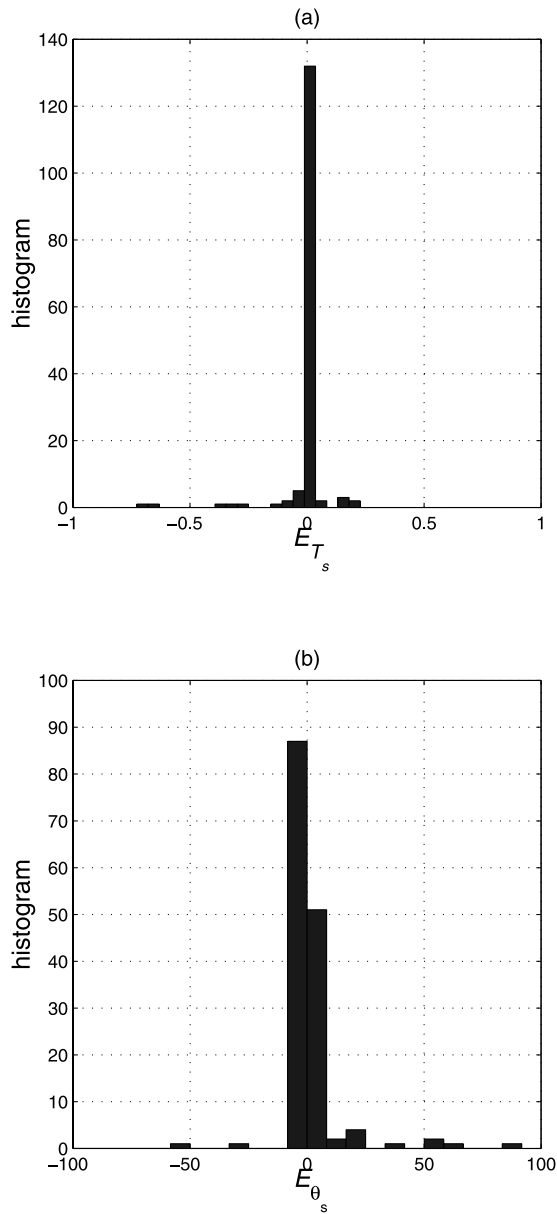


Figure 4. Validation of equations (10) and (11). (a) Histogram of conditioned partial derivative of E with respect to T_s on given $R_n - G$, E_{T_s} , with a mean $\mu_{E_{T_s}} = -0.012$ and a standard deviation $\sigma_{E_{T_s}} = 0.098$. (b) Histogram of conditioned partial derivative of E with respect to θ_s on given $R_n - G$, E_{θ_s} , with a mean $\mu_{E_{\theta_s}} = 1.019$ and a standard deviation $\sigma_{E_{\theta_s}} = 18.367$. In the captions, $E_H = \partial E / \partial H$, $G_{T_s} = \partial G / \partial T_s$, etc. Data from the HAPEX-SAHEL experiment shown in Figure 1. See color version of this figure in the HTML.

[38] The parameter restriction analysis includes the following steps:

[39] 1. Divide the entire multidimensional domain of observed variables, θ_s , T_s , H , v_d , and R , into N subdomains assuming that E can be approximated by piecewise linear functions over the subdomains.

[40] 2. Estimate a linear regression function E^i of the unrestricted model in equation (27) for all subdomains $i = 1, 2, \dots, N$.

[41] 3. Calculate the unrestricted residual sum of squared errors,

$$RSS_u = \sum_{i=1}^N (E^{io} - E^i)^2,$$

where E^{io} is the observed value of E .

[42] 4. Estimate a linear regression function E^i of the restricted model in equation (1) for the same subdomains. This is called restricted since the regression coefficient of v_d is restricted to be zero.

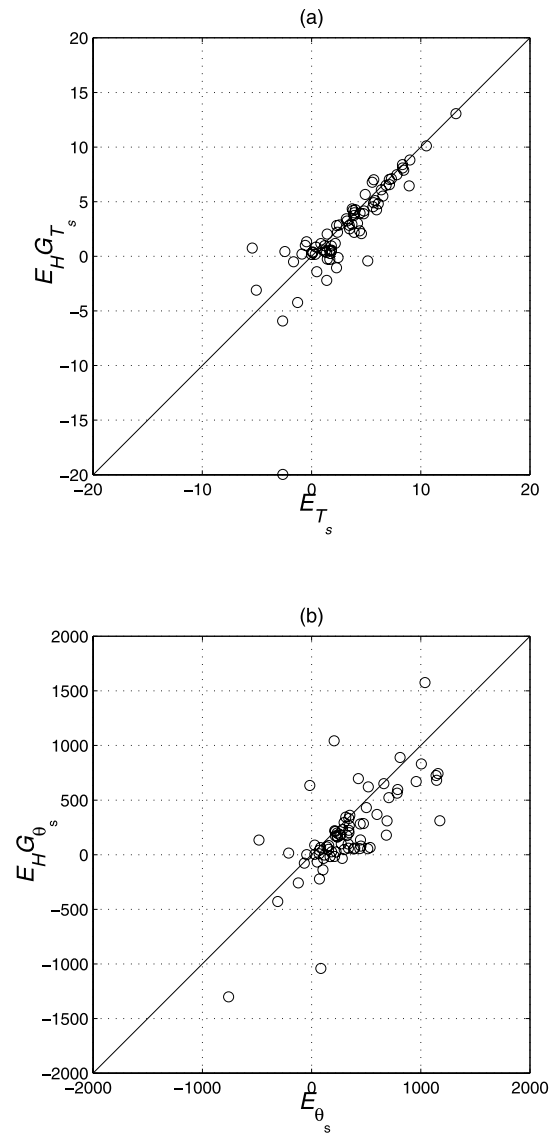


Figure 5. Validation of equations (18) and (19). (a) Mean regression slope $\bar{b} = 0.998$, 95% confidence interval of \bar{b} (1.189, 0.808). (b) Validation of equation (19), mean regression slope $\bar{b} = 0.747$, 95% confidence interval of \bar{b} (0.959, 0.529). The statistics are obtained by the analysis of linear functional relationships [e.g., *Davies and Goldsmith*, 1984]. Data from the HAPEX-SAHEL experiment shown in Figure 1. See color version of this figure in the HTML.

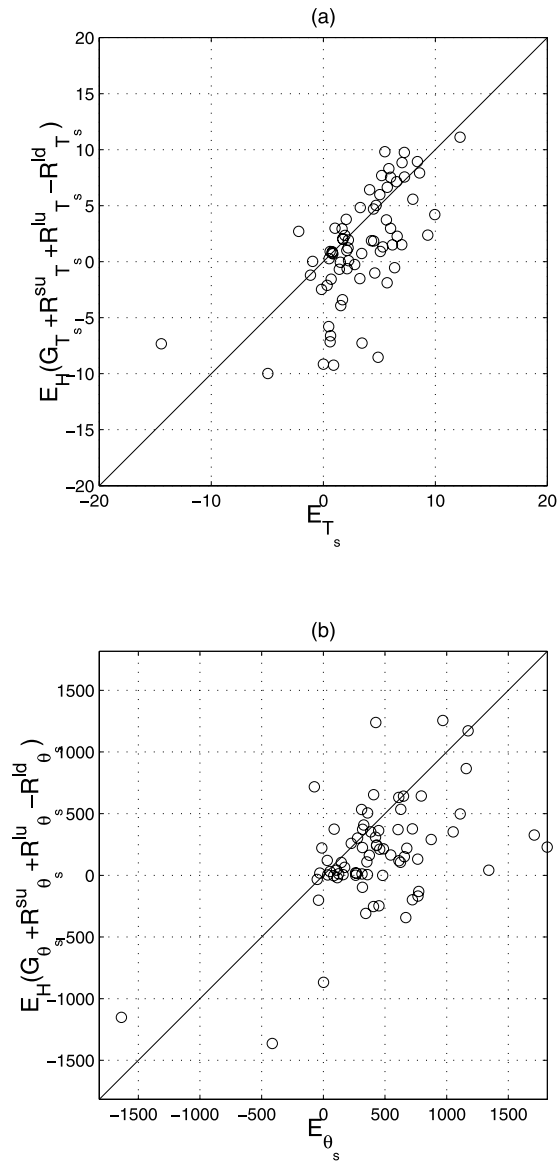


Figure 6. The hypothesis test for the case of given R^{sd} . (a) Validation of equation (22): $\bar{b} = 1.124$, 95% confidence interval of \bar{b} (1.399, 0.862). (b) Validation of equation (23): $\bar{b} = 0.266$, 95% confidence interval of \bar{b} (0.445, 0.07). Data from the HAPEX-SAHEL experiment shown in Figure 1. See color version of this figure in the HTML.

[43] 5. Calculate the restricted residual sum of squared errors,

$$RSS_r = \sum_{i=1}^N (E^{io} - E^i)^2.$$

[44] 6. Form a test statistic

$$\omega = \left(\frac{RSS_r}{RSS_u} - 1 \right) \frac{T - k}{s},$$

where T is the number of observations used in calculating the regression coefficients, k is the number of regressors in the unrestricted model (i.e., five in equation (1)), and s is the number of regressors restricted to zero in the restricted

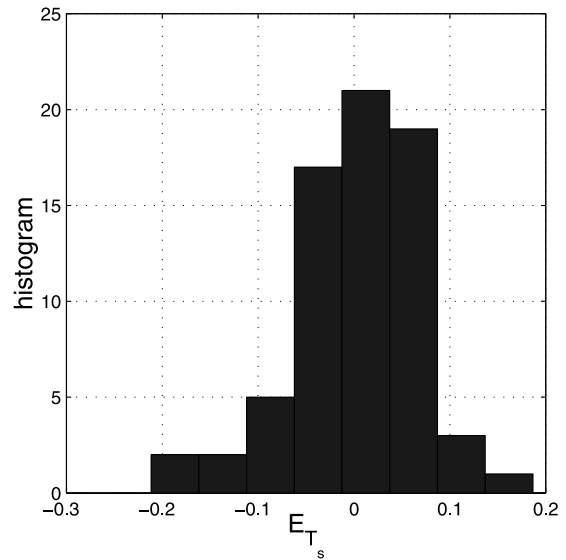


Figure 7. The hypothesis test for the case of given $R_n - G$. Validation of equation (10): histogram of $\partial E / \partial T_s$ ($\mu = 0.0043$ and $\sigma = 0.069$). Data from SGP97 experiment shown in Figure 2. See color version of this figure in the HTML.

model (i.e., one in equation (27)) for each of the N subdomains.

[45] It can be shown [e.g., Pindyck and Rubinfeld, 1998, p. 134] that ω follows the F distribution, $F_{s, T-k}$, under the null hypothesis. Large ω indicates a large decrease in the predictive capability of the restricted model relative to the disadvantage built in by having one fewer regressor. A p value associated with the ω can be defined as

$$p = 1 - \int_{-\infty}^{\omega} F_{s, T-k}(x) dx,$$

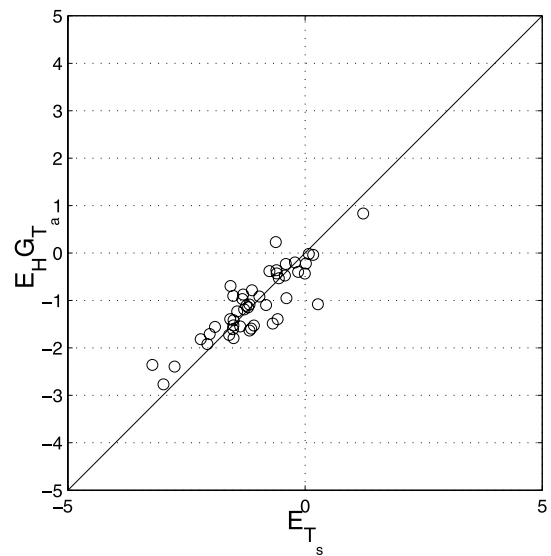


Figure 8. The hypothesis test for the case of given R_n . Validation of equation (18): $\bar{b} = 0.98$, 95% confidence interval of $\bar{b} = [1.18, 0.77]$. Data from SGP97 experiment shown in Figure 2. See color version of this figure in the HTML.

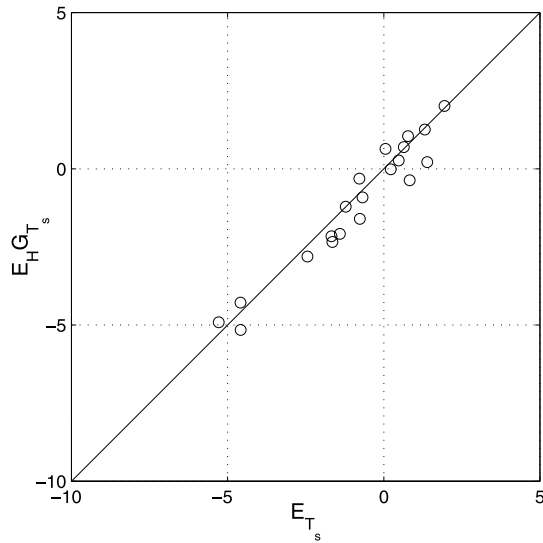


Figure 9. The hypothesis test for the case of given R_n . Validation of equation (18): $\bar{b} = 1.15$, 95% confidence interval of $\bar{b} = [1.39, 0.79]$. Data from the University of California, Davis, experiment shown in Figure 3. See color version of this figure in the HTML.

which forms a population with a uniform distribution between 0 and 1 under the null hypothesis. Hence the null hypothesis should be rejected at the significance level α when $p < \alpha$ for an individual subdomain where the linear regression is performed.

[46] Now we use a standard meta-analysis procedure to create an overall p value based on the individual p values, p_i , for each of the N subdomains. To do so, we introduce a new statistic Γ ,

$$\Gamma = \sum_{i=1}^N \ln\left(\frac{1}{p_i^2}\right).$$

It turns out that Γ follows the χ_{2N}^2 distribution under the null hypothesis. The overall p value, \mathcal{P} , can be defined as

$$\mathcal{P} = 1 - \int_0^{\Gamma} \chi_{2N}^2(x) dx,$$

so that the null hypothesis should be rejected at the significance level α when $\mathcal{P} < \alpha$ for the entire domain of the observed independent variables.

[47] Using the data shown in Figure 1 (v_d not shown), we divide the observed variables into $N = 50$ subdomains. Here we use the daytime data points corresponding to $R_n > 0$ when significant evaporation occurs. The overall p value is found to be $\mathcal{P} = 0.17$, suggesting that the null hypothesis should not be rejected at, say, the 5% significance level. The hypothesis is only rejected at the 17% or higher level, which is unusually high in practice. The result is robust in terms of N . In fact, the overall p value is much greater for $N = 10$ (fewer fitting parameters), $\mathcal{P} = 0.58$, stronger evidence that hypothesis H_0 should be accepted. On the basis of this analysis, we conclude that water vapor deficit does not significantly influence evaporation, and hence equation (1)

suffices. This result is consistent with a recent sensitivity study by *Lakshmi and Suskind* [2001], who also found that evaporation is not sensitive to atmospheric humidity.

3.5. Discussion

[48] The validity of equation (1) is arguably attributed to the two distinct intrinsic timescales associated with the dynamics of land-atmosphere interaction: $\sim 10^{-2}$ s of turbulent eddies in the atmosphere and $\sim 10^3$ s of molecular diffusion in the soil. Because of the wide gap between the two timescales, the land surface and the atmosphere are in the state of (thermal) quasi-equilibrium at all times under usual synoptic conditions. When the equilibrium is perturbed by the diurnal cycle of radiative forcing and/or changing meteorological environment, a new equilibrium will be established very rapidly due to the effectiveness of turbulent transfer. Therefore the surface fluxes are adequately described by the thermodynamic and hydrologic states of the surface.

4. An Application

[49] Up to this point, the analysis has been independent of the functional form of evaporation. No model is assumed. Now we demonstrate how the theory can help in further understanding the existing models of evaporation. Using the Priestley-Taylor formula for potential evaporation as an example, we will show that the extremum principle will lead to an estimate of the empirical coefficient in the Priestley-Taylor formula consistent with the consensus.

[50] *Priestley and Taylor* [1972] had shown that potential evaporation E_p (evaporation under the condition of unlimited water supply) may be expressed to a good approximation as

$$E_p = \alpha \frac{R_n - G}{1 + \gamma/\Delta}, \quad (28)$$

where Δ is the derivative of saturated vapor pressure with respect to temperature and γ is the psychrometric constant. The α is an empirical parameter assumed to be constant with a “best” value of 1.26. It has been found that the values of α in equation (28) from various field experiments do vary within a narrow range. Here we demonstrate that this variability is consistent with that predicted by our theory.

[51] E_p in equation (28) can be written as a function of H and T_s by using equation (20),

$$E_p = \frac{\alpha H}{1 + \gamma/\Delta - \alpha}. \quad (29)$$

Equation (18) must be satisfied if E_p is maximum. Note that in equation (29) H could be negative when α is greater than $1 + \gamma/\Delta$. Substituting equation (29) into equation (18) gives the solution of α ,

$$\alpha = 1 + \frac{\gamma}{\Delta} + H \frac{d}{dT_s} \left(\frac{\gamma}{\Delta} \right) \left(\frac{dG}{dT_s} \right)^{-1}. \quad (30)$$

Contrary to the earlier studies where α has to be derived as the regression coefficient according to equation (28) using observed E_p , G , and T_s , the extremum principle allows α to

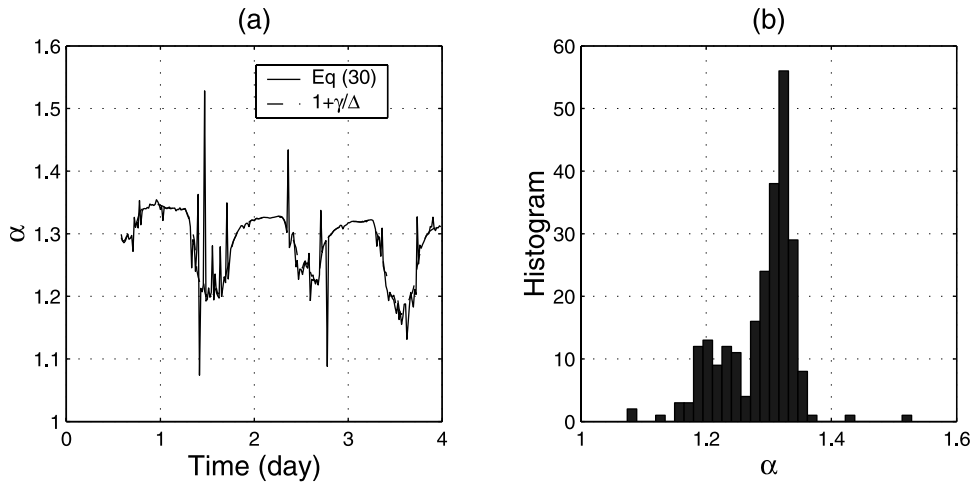


Figure 10. (a) Sequential series of the calculated α from equation (30). (b) Histogram of the calculated α . The $m_\alpha = 1.287$, $\sigma_\alpha = 0.058$. Data of T_s , G , and H from HAPEX-SAHEL experiment at the Southern Tiger Bush site, 28–31 August 1992. See color version of this figure in the HTML.

be derived independent of E_p . The solution of α in equation (30) is essentially identical to that obtained using the classic Penman's equation [Eichinger *et al.*, 1996] and that derived using a boundary layer model [de Bruin, 1983]. Since the third term in equation (30) is often small, α in equation (30) is essentially equal to that under the isothermal condition (i.e., zero sensible heat flux) [Eagleson, 2002, p. 162].

[52] Note that α in equation (28) is supposed as a constant. Therefore equation (30) should be understood as a constraint on the surface variables T_s , H , and G , rather than a functional dependence of α on these variables. Since G is a known function of T_s , equation (30) implies that H must be a specific function of T_s as well. This restrictive condition on H results from the empirical nature of the Priestley-Taylor formula and hence is not expected to be exact. Nonetheless, equation (30) does provide a rationale for estimating α . Practically, the theoretical imperfection in Priestley-Taylor's theory does not seem to hurt its usefulness in modeling potential evaporation. Such fortuity comes from the limited variability in α under natural conditions.

[53] Figure 10 displays the estimated α according to equation (30). Measurements of T_s , H , and G over a saturated soil over the period of 28–31 August 1992 were collected (not shown) during the HAPEX-SAHEL field experiment at the same location as the data shown in Figure 1. Several features are evident. First, α varies between 1.1 and 1.4 with a mean value of 1.287, remarkably close to the widely accepted value of 1.26. Second, α moves diurnally with a rather uniform value about 1.33 over nighttime and down to about 1.2 during daytime. Third, α is dominated by the first two terms in equation (30), which not only explains why α from various studies consistently fluctuates around the 1.26 level, but also why Priestley-Taylor's formula sometimes predicts an E_p greater than the available energy $R_n - G$. The above analysis further suggests that although practically useful, Priestley-Taylor's formula is fundamentally flawed in the sense that there is no unique universal constant α that gives the maximum (potential) evaporation at all times.

[54] The success of the Priestley-Taylor equation (although deficient) serves as evidence that the near-surface

vapor pressure is not a “free” external variable that can be arbitrarily imposed. Recall that the Priestley-Taylor equation, or more generally Penman's equation, is derived by conveniently separating the vapor pressure gradient term into a saturation gradient term evaluated at the surface and a saturation deficit term prescribed at an arbitrary finite distance above the surface. Priestley and Taylor realized that the saturation deficit term in Penman's equation can be eliminated by introducing an empirical parameter. Their finding implies that the near-surface saturation deficit is closely correlated with the surface saturation gradient. The “drying power” seems to be created by the internal feedback of the land-atmosphere interaction system rather than by the external atmospheric conditions. If this is indeed the case, vapor pressure deficit would be a redundant variable in formulating E . That leads to the conclusion that E expressed in equation (1) is more than merely a convenient alternative mathematical formulation.

[55] There are scattered publications supporting the argument that evaporation is reasonably insensitive to atmospheric humidity. Brutsaert [1982, p. 168] offered an analytical solution of E expressed as a function of specific humidity and its infinitesimal gradient at the surface for the case of advection from a relatively dry surface over a wet surface of finite dimension. The implication of that example is that E would be the same for any humidity profiles at finite height as long as the local gradients of the humidity profiles are identical at the surface. This theoretical study is consistent with observations. Parlange and Katul [1992] conducted a field experiment to investigate the evaporation over a saturated soil. They noted (p. 131) that “because of an increase in the afternoon wind speed (5 m s^{-1}), large-scale advection was important even though the minimum air relative humidity could be considered high (52%).” Their result may be interpreted as that the enhanced evaporation is caused by the increased wind speed (i.e., stronger transport mechanism), rather than by the reduced atmospheric humidity. The so-called “oasis effect” (i.e., enhanced evaporation over an isolated wet and cool plot surrounded by dry and warm land) [e.g., Miller, 1977, p. 285] is often observed during windy days [Tsukamoto *et al.*, 1995],

suggesting that evaporation is directly responding to the transport mechanism due to the strong wind rather than to the change in the atmospheric moisture. *Ye and Pielke* [1993] compared several commonly used humidity gradient based evaporation algorithms. They concluded that the model more consistent with the gradient-flux theory gives poorer estimates of evaporation. Recently, *Lakshmi and Susskind* [2001] investigated regional evaporation using remote sensing observations and found little sensitivity of evaporation to the near-surface atmospheric humidity. These studies offer worthy evidence for a critical evaluation of the traditional view on the effect of atmospheric humidity on evaporation.

5. Conclusions

[56] This study leads to two major findings: (1) Evaporation is always maximized in balancing the surface energy budget, and (2) evaporation, well described by the surface state variables, is insensitive to water vapor pressure deficit at a finite height.

[57] The proposed extremum principle of evaporation has two distinctive features. First, the theory builds on a fundamental concept of thermodynamic equilibrium. The proposition that the land-atmosphere interaction system evolves following an optimal path toward a potential liquid-vapor equilibrium is motivated by many well-established maximum principles that exist in the natural physical systems. Second, the development of the theory is independent of turbulent transport and radiative transfer models. Consequently the extremum principle leads to a generic physically based description of the surface energy budget and the surface temperature and soil moisture states. We hope this paper will inspire more research to further evaluate these findings.

[58] It is important to emphasize that the second conclusion does not contradict the concept of down-gradient transport of water vapor. Exclusion of atmospheric humidity in our formulation of evaporation by no means implies a weakened land-atmosphere interaction. We view it as an indication of strong land-atmosphere interaction. Such a close coupling implies that the signal of atmospheric humidity conditions is inherent in the surface variables like soil moisture and temperature. The gradients of temperature and humidity at the surface associated with the fluxes of heat and water vapor are driven and maintained by the demand of maximum evaporation toward a potential liquid-vapor equilibrium.

[59] From a practical perspective, the extremum principle supports a unified and versatile framework for modeling land surface processes. Although developing a new land surface scheme is beyond the scope of this paper, the proposed theory offers fresh possibilities to do so. "Unified" here means that the theory makes it possible to parameterize evaporation (and the other heat fluxes) diagnostically for the entire range of soil moisture without separating the soil-controlled stage from the climate-controlled stage. The surface heat fluxes as the solution of the governing equations will be guaranteed to balance the energy budget. Surface temperature and soil moisture will be product rather than input as in many commonly used hydrological models. Such formulated land surface schemes will distinguish themselves, among other things,

by allowing the surface fluxes, temperature, and soil moisture to be derived without solving prognostic equations as in the popular force-restore method and the like. "Versatile" means that the extremum principle is generic and independent of turbulent transport models. Nonparametric formulation of the theory will allow an objective judgment of the existing diagnostic and/or prognostic models that often produce inconsistent estimates of the surface heat fluxes. One possible application is to use the governing equations as constraints on the estimation of model parameters. A particularly attractive feature of the theory is the minimum input of radiative energy fluxes, which makes it a suitable tool for remote sensing of hydrologic cycles. We expect our proposed theory to be potentially helpful to the study of large-scale hydrology as remote sensing observations are becoming more readily available with ever improving quality.

[60] **Acknowledgments.** This work was supported by NSF grants EAR-9804996 and EAR-0309594 and a NASA TRMM project under grant NAG5-3726. We benefited enormously from discussions with Dara Entekhabi and Alar Toomre of MIT. We are grateful to Gabriel Katul of Duke University and Marc Parlange of Johns Hopkins University for preparing the UC Davis field measurement data used in our analysis. We thank our colleagues Steven Margulis, Enrique Vivoni, Frédéric Chagnon, and Susan Dune for their assistance during this study. The data sets used in this study are from the HAPEX-SAHEL Information System and SGP97 data archive where the data products are made available to the public by the scientists of the field campaigns. We sincerely thank Marc Parlange and William Eichinger and an anonymous reviewer, whose comments greatly improved the quality of this paper.

References

- Bouchet, R. J. (1963), Evapotranspiration reele et potentielle, signification climatique, in *General Assembly of Berkeley, Red Book 62*, pp. 134–142, Int. Assoc. of Hydrolol. Sci., Gentbrugge, Belgium.
- Bras, R. L. (1990), *Hydrology*, 643 pp., Addison-Wesley-Longman, Reading, Mass.
- Brutsaert, W. (1982), *Evaporation Into the Atmosphere: Theory, History and Applications*, 299 pp., Kluwer Acad., Norwell Mass.
- Brutsaert, W., and M. B. Parlange (1998), Hydrologic cycle explains the evaporation paradox, *Nature*, 396, 30.
- Brutsaert, W., and H. Sticker (1979), An advection-aridity approach to estimate actual regional evapotranspiration, *Water Resour. Res.*, 15(2), 443–450.
- Businger, J. A., J. C. Wyngaard, Y. Izumi, and E. F. Bradley (1971), Flux profile relationships in the atmospheric surface layer, *J. Atmos. Sci.*, 28, 181–189.
- Davies, O. L., and P. L. Goldsmith (1984), *Statistical Methods in Research and Production*, Addison-Wesley-Longman, Reading, Mass.
- de Bruin, H. A. R. (1983), A model for the Priestley-Taylor parameter α , *J. Clim. Appl. Meteorol.*, 22, 573–578.
- Delworth, T. L., and S. Manabe (1989), The influence of soil wetness on near-surface atmospheric variability, *J. Clim.*, 2, 1447–1462.
- Desborough, C. E., A. J. Pitman, and P. Irannejad (1996), Analysis of the relationship between bare soil evaporation and soil moisture simulated by 13 land surface schemes for a simple non-vegetated site, *Global Planet. Change*, 13, 47–56.
- de Vries, D. A. (1963), Thermal properties of soils, in *Physics of Plant Environment*, pp. 210–235, North-Holland, New York.
- Dyer, A. J., and F. J. Maher (1965), Automatic eddy-flux measurement with the evapotron, *J. Appl. Meteorol.*, 4, 622–625.
- Eagleson, P. S. (2002), *Ecohydrology: Darwinian Expression of Forest Form and Function*, 443 pp., Cambridge Univ. Press, New York.
- Edlfsen, N. E., and B. C. Anderson (1943), Thermodynamics of soil moisture, *Hilgardia*, 15(2), 31–298.
- Eichinger, W. E., M. B. Parlange, and H. Sticker (1996), On the concept of equilibrium evaporation and the value of the Priestley-Taylor coefficient, *Water Resour. Res.*, 32(1), 161–164.
- Goutorbe, J.-P., et al. (1994), HAPEX-Sahel: A large-scale study of land-atmosphere interactions in the semi-arid tropics, *Ann. Geophys. Atmos. Hydrospheres Space Sci.*, 12(1), 53–64.

- Henderson-Sellers, A., P. Irannejad, K. McGuffie, and A. Pitman (2003), Predicting land-surface climates: Better skills or moving targets?, *Geophys. Res. Lett.*, 30(14), 1777, doi:10.1029/2003GL017387.
- Idso, S. B., R. D. Jackson, R. J. Reginato, B. A. Kimball, and F. S. Nakayama (1975), The dependence of bare soil albedo on soil water content, *J. Appl. Meteorol.*, 14(1), 109–113.
- Jackson, R. D., S. B. Idso, and R. J. Reginato (1976), Calculation of evaporation rates during the transition from energy-limiting to soil-limiting phases using albedo data, *Water Resour. Res.*, 12(1), 23–26.
- Kanemasu, E. T., et al. (1992), Surface flux measurements in FIFE: An overview, *J. Geophys. Res.*, 97(D17), 18,547–18,555.
- Katul, G. G., and M. B. Parlange (1992), A Penman-Brutsaert model for wet surface evaporation, *Water Resour. Res.*, 28(1), 121–126.
- Kim, C. P., and D. Entekhabi (1997), Examination of two methods for estimating regional evaporation using a coupled mixed layer and land surface model, *Water Resour. Res.*, 33(9), 2109–2116.
- Kondepudi, D., and I. Prigogine (1998), *Modern Thermodynamics*, 486 pp., John Wiley, Hoboken, N. J.
- Lakshmi, V., and J. Susskind (2001), Utilization of satellite data in land surface hydrology: Sensitivity and assimilation, *Hydrol. Processes*, 15(5), 877–892.
- Mahrt, L., and M. Ek (1984), The influence of atmospheric stability on potential evaporation, *J. Clim. Appl. Meteorol.*, 23, 222–234.
- McNaughton, K. G., and T. W. Spriggs (1986), A mixed-layer model for regional evaporation, *Boundary Layer Meteorol.*, 34, 243–262.
- Miller, D. H. (1977), *Water at the Surface of the Earth*, 557 pp., Academic, San Diego, Calif.
- Obukhov, A. M. (1946), Turbulence in an atmosphere of non-homogeneous temperature, *Trans. Inst. Theor. Geophys. USSR*, 1, 95–115.
- Ozawa, H., A. Ohmura, R. D. Lorenz, and T. Pujol (2003), The second law of thermodynamics and the global climate system: A review of the maximum entropy production principle, *Rev. Geophys.*, 41(4), 1018, doi:10.1029/2002RG000113.
- Parlange, M. B., and G. G. Katul (1992), An advection-aridity evaporation model, *Water Resour. Res.*, 28(1), 127–132.
- Penman, H. L. (1948), Natural evaporation from open water, bare soil, and grass, *Proc. R. Soc. London A*, 193, 120–145.
- Pielke, R. A., G. Marland, R. A. Betts, T. N. Chase, J. L. Eastman, J. O. Niles, D. D. S. Niyogi, and S. W. Running (2002), The influence of land-use change and landscape dynamics on the climate system: Relevance to climate-change policy beyond the radiative effect of greenhouse gases, *Philos. Trans. R. Soc. London, Ser. A*, 360, 1705–1719.
- Pindyck, R. S., and D. L. Rubinfeld (1998), *Econometric Models and Economic Forecasts*, 643 pp., McGraw-Hill, New York.
- Prausnitz, J. M. (1969), *Molecular Thermodynamics of Fluid-Phase Equilibrium*, 523 pp., Prentice-Hall, Upper Saddle River, N. J.
- Priestley, C. H. B., and R. J. Taylor (1972), On the assessment of surface heat flux and evaporation using large scale parameters, *Mon. Weather Rev.*, 100, 81–92.
- Raupach, M. R. (2001), Combination theory and equilibrium evaporation, *Q. J. R. Meteorol. Soc.*, 127, 1149–1181.
- Roderick, M. L., and G. D. Farquhar (2002), The cause of decreased pan evaporation over the past 50 years, *Science*, 298, 1410–1411.
- Salvucci, G. D. (1997), Soil and moisture independent estimation of stage-two evaporation from potential evaporation and albedo or surface temperature, *Water Resour. Res.*, 33(1), 111–122.
- Schulze, R., H. Holling, and D. Boehning (2003), *Meta-Analysis: New Developments and Applications in Medical and Social Sciences*, 288 pp., Hogrefe and Huber, Cambridge, Mass.
- Sellers, P. J., F. G. Hall, G. Arsar, D. E. Strebel, and R. E. Murphy (1992), An overview of the First International Satellite Land Surface Climatology Project (ISLSCP) Field Experiment (FIFE), *J. Geophys. Res.*, 97(D17), 18,345–18,371.
- Sieniutycz, S., and P. Salamon (1990), *Nonequilibrium Theory and Extremum Principles*, 547 pp., Taylor and Francis, Philadelphia, Pa.
- Stull, R. B. (1988), *An Introduction to Boundary Layer Meteorology*, 666 pp., Kluwer Acad., Norwell, Mass.
- Tsukamoto, O., K. Sahashi, and J. Wang (1995), Heat budget and evapotranspiration at an oasis surface surrounded by desert, *J. Meteorol. Soc. Jpn.*, 73(5), 925–935.
- Wang, J., and R. L. Bras (1999), Ground heat flux estimated from surface soil temperature, *J. Hydrol.*, 216, 214–226.
- Weinstock, R. (1952), *Calculus of Variations With Applications to Physics and Engineering*, 326 pp., McGraw-Hill, New York.
- Ye, Z., and R. A. Pielke (1993), Atmospheric parameterization of evaporation from non-plant-covered surfaces, *J. Appl. Meteorol.*, 32(7), 1248–1258.

R. L. Bras and J. Wang, Department of Environmental Engineering, Massachusetts Institute of Technology, Cambridge, MA 02139, USA. (jfwang@mit.edu)

G. D. Salvucci, Department of Earth Sciences and Geography, Boston University, Boston, MA 02215, USA.